Research

New Phytologist

The complexity of intercellular localisation of alkaloids revealed by single-cell metabolomics

Kotaro Yamamoto[1,2], Katsutoshi Takahashi[3], Lorenzo Caputi[2], Hajime Mizuno[4], Carlos E. Rodriguez-Lopez[2], Tetsushi Iwasaki[1], Kimitsune Ishizaki[1], Hidehiro Fukaki[1], Miwa Ohnishi[1], Mami Yamazaki[5], Tsutomu Masujima[6†], Sarah E. O'Connor[2] and Tetsuro Mimura[1]

[1]Department of Biology, Graduate School of Science, Kobe University, Kobe, Hyogo 657-8501, Japan; [2]Department of Biological Chemistry, John Innes Centre, Norwich Research Park, Norwich, NR4 7UH, UK; [3]Biotechnology Research Institute for Drug Discovery, National Institute of Advanced Industrial Science and Technology (AIST), Koutou-ku, Tokyo 135-0064, Japan; [4]Laboratory of Analytical and Bio-Analytical Chemistry, School of Pharmaceutical Sciences, University of Shizuoka, Shizuoka, Shizuoka 422-8526, Japan; [5]Graduate School of Pharmaceutical Sciences, Chiba University, Chiba, Chiba 263-8522, Japan; [6]Quantitative Biology Centre (QBiC), RIKEN, Suita, Osaka 565-0874, Japan

Author for correspondence:
Tetsuro Mimura
Tel: +81 78 803 5708
Email: mimura@kobe-u.ac.jp

Received: *15 January 2019*
Accepted: *19 June 2019*

New Phytologist (2019) **224:** 848–859
doi: 10.1111/nph.16138

Key words: alkaloid, Apocynaceae, *Catharanthus roseus*, idioblast cell, Imaging MS, laticifer cell, secondary metabolism, single-cell MS.

Summary

- *Catharanthus roseus* is a medicinal plant well known for producing bioactive compounds such as vinblastine and vincristine, which are classified as terpenoid indole alkaloids (TIAs). Although the leaves of this plant are the main source of these antitumour drugs, much remains unknown on how TIAs are biosynthesised from a central precursor, strictosidine, to various TIAs *in planta*.
- Here, we have succeeded in showing, for the first time in leaf tissue of *C. roseus*, cell-specific TIAs localisation and accumulation with 10 μm spatial resolution Imaging mass spectrometry (Imaging MS) and live single-cell mass spectrometry (single-cell MS).
- These metabolomic studies revealed that most TIA precursors (iridoids) are localised in the epidermal cells, but major TIAs including serpentine and vindoline are localised instead in idioblast cells. Interestingly, the central TIA intermediate strictosidine also accumulates in both epidermal and idioblast cells of *C. roseus*. Moreover, we also found that vindoline accumulation increases in laticifer cells as the leaf expands.
- These discoveries highlight the complexity of intercellular localisation in plant specialised metabolism.

Introduction

Terpenoid indole alkaloids (TIAs) constitute one of the largest groups of alkaloids, many of which have potent biological functions and pharmaceutical importance. *Catharanthus roseus* (L.) G. Don (Apocynaceae) is one of the best-characterised TIA containing plants that produces many commercially valuable TIAs, for example antitumour drugs such as vinblastine and vincristine (Van der Heijden *et al.*, 2004; Gigant *et al.*, 2005; Kavallaris, 2010). Extensive studies have revealed that > 130 TIAs are produced from strictosidine, which is the central precursor for all TIAs in *C. roseus* (Fig. 1a; Verma *et al.*, 2012).

TIA metabolism in *C. roseus* is believed to start from internal phloem-associated parenchyma cells (IPAP cells), proceeding to epidermal cells and then to both idioblast cells and laticifer cells where vindoline and other highly derivatised TIAs are believed to be accumulated (Yoder & Mahlberg, 1976; Mahroug *et al.*, 2006; Dugé de Bernonville *et al.*, 2015). Cell type-specific localisation of TIA metabolic pathways have been primarily inferred from the results of *in situ* RNA hybridisation and immunocytochemical localisation of enzymes of TIA metabolic pathways (St-Pierre *et al.*, 1999; Burlat *et al.*, 2004; Mahroug *et al.*, 2007; Guirimand *et al.*, 2011; Pan *et al.*, 2016). The current understanding, mainly deduced from such studies on leaf tissues, is that secoiridoid metabolism begins in IPAP cells and that the late-stage iridoid loganic acid is produced in IPAP cells and then transported to epidermal cells (Burlat *et al.*, 2004; Dugé de Bernonville *et al.*, 2015) where further downstream biosynthesis involving the iridoid secologanin and strictosidine occurs (Fig. 1a,c). Associated TIA intermediates are also accumulated in the same cells (Burlat *et al.*, 2004; Dugé de Bernonville *et al.*, 2015). Finally, a TIA intermediate, desacetoxyvindoline moves to the idioblast or laticifer cells and late-stage TIAs are accumulated in the vacuoles of those cells (Yoder & Mahlberg, 1976; Burlat *et al.*, 2004; Dugé de Bernonville *et al.*, 2015).

While *in situ* RNA hybridisation and immunocytochemical localisation support this model, cellular localisation of actual metabolites, however, has not yet been realised. Recently we have reported the cell-specific localisation of intermediates of TIA

†This article is dedicated to the late Prof. Tsutomu Masujima who is one of authors and was a prominent scientist who had developed a single-cell analysis of metabolites.

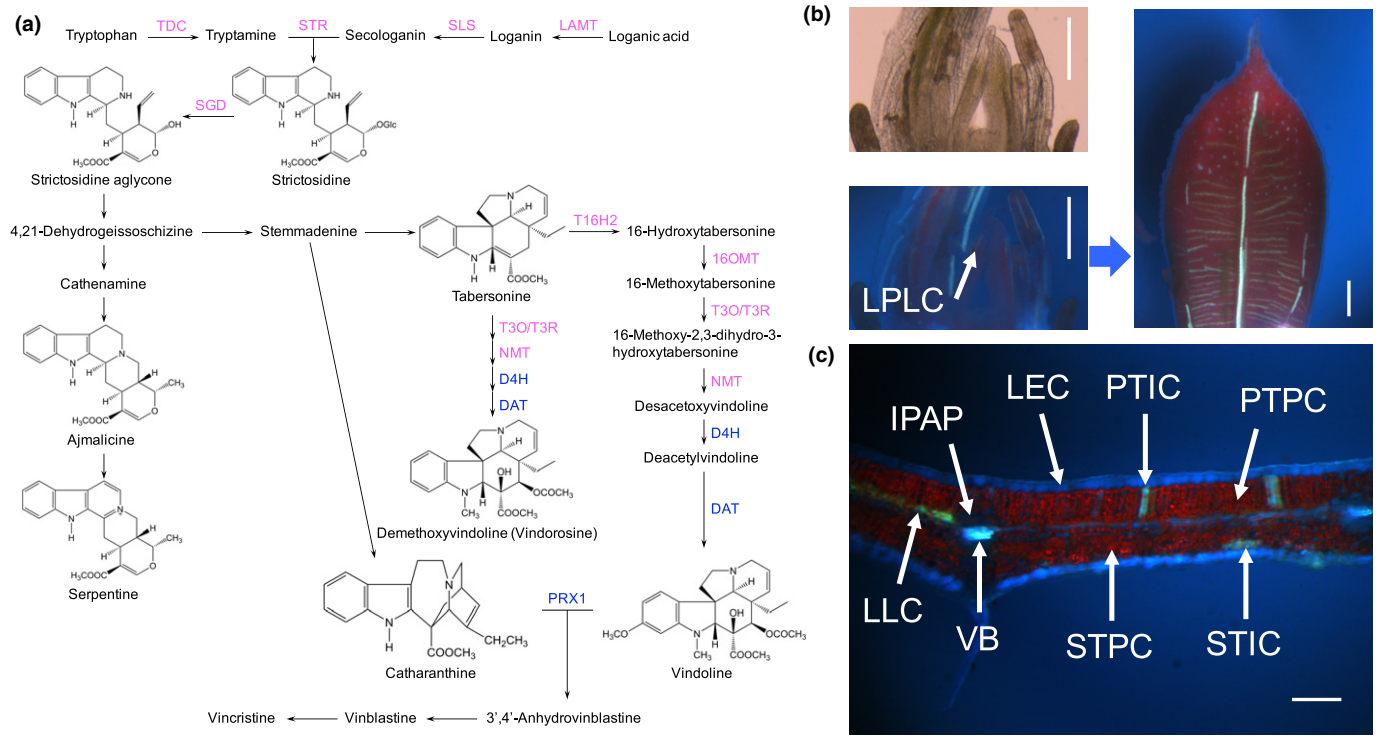

Fig. 1 Terpenoid indole alkaloid (TIA) biosynthetic pathway and localisation of idioblast cells and laticifer cells in *Catharanthus roseus* leaf tissue. (a) Speculated TIA metabolic pathway in *C. roseus*. Purple font represents TIA enzymes localised in epidermal cells. Blue font represents TIA enzymes localised in idioblast cells and laticifer cells. LAMT, loganic acid *O*-methyltransferase; SLS, secologanin synthase; TDC, tryptophan decarboxylase; STR, strictosidine synthase; SGD, strictosidine β-glucosidase; T16H2, tabersonine 16-hydroxylase 2; 16OMT, 16-hydroxytabersonine *O*-methyltransferase; T3O, tabersonine 3-oxygenase; T3R, tabersonine 3-reductase; NMT, 16-methoxy-2,3-dihydro-3-hydroxy-tabersonine *N*-methyltransferase; D4H, desacetoxyvindoline 4-hydroxylase; DAT, deacetylvindoline 4-*O*-acetyltransferase; PRX1, peroxidase 1. (b) Shoot apical meristem and young leaf (*c.* 2 mm). Leaf expansion from leaf primordium. These figures show a bright field image and fluorescence images excited with UV. Bars, 200 μm. (c) Cross-section of *C. roseus* young leaf (*c.* 1 cm). This figure shows a fluorescence image following UV light excition. Bar, 100 μm. LPLC, leaf primordium laticifer cell; IPAP, internal phloem-associated parenchyma cell; LEC, leaf epidermal cell; PTPC, palisade tissue parenchyma cell; STPC, spongy tissue parenchyma cell; PTIC, palisade tissue idioblast cell; STIC: spongy tissue idioblast cell; LLC, leaf laticifer cell; VB, vascular bundle.

metabolism in the stem tissue in *C. roseus* using Imaging mass spectrometry (Imaging MS) and live single-cell mass spectrometry (single-cell MS) (Yamamoto *et al.*, 2016). In our measurements, loganin and secologanin are localised in epidermal cells, consistent with the reported localisation of iridoid biosynthetic enzymes (LAMT, loganate *O*-methyltransferase; SLS, secologanin synthase) (Murata *et al.*, 2008; Guirimand *et al.*, 2011). Most TIAs including strictosidine and serpentine, however, localised in both idioblast cells and laticifer cells of *C. roseus* stem tissue, which is different from the above hypothesis suggesting that these compounds are produced in epidermal cells (Yamamoto *et al.*, 2016). The new aspect of localisation of TIAs in *C. roseus* stem tissue led us to hypothesise that the TIA pathway localisation in the stem tissue might be different in the leaf tissue. So far, the actual localisation of TIA intermediates at the cellular level in leaf tissues has not been directly measured in *C. roseus* because of the technical challenges associated with measuring smaller leaf cells. However, as leaves are a commercially important source of alkaloids, it is critical to understand the localisation patterns in this tissue (Fig. 1; O'Keefe *et al.*, 1997).

In the present study, we have applied state-of-the-art methods of Imaging MS and single-cell MS for detecting metabolites *in situ* at the cellular level in leaf tissue of *C. roseus* as well as the stem tissue (Mizuno *et al.*, 2008; Fujii *et al.*, 2015; Takahashi *et al.*, 2015; Yamamoto *et al.*, 2016). By improving methods of laser irradiation for Imaging MS and of micro-capillary and video-assisted system for single-cell MS, we successfully elucidated single-cell-specific TIA localisation in the leaf tissue of *C. roseus*.

Overall, the alkaloid localisation in stem and leaf was largely similar. The exceptions were strictosidine, which localised in idioblast cells in stem, but was found in both epidermal cells and idioblast cells in leaf, and vindoline, as well as certain vindoline intermediates, accumulated in idioblast cells in leaf, whereas in stem we could not detect vindoline except for vindorosine in idioblast cells. We detected precisely vindoline related intermediates from the data of VIGS and single-cell MS in the laticifer cell in leaf primordia and leaf tissues thus providing proof of concept for combining gene silencing with metabolite imaging. In summary, we succeeded in detecting in the present study that there are subtle but significant changes in biosynthetic capacity between stem and leaf. Our results highlight the complex localisation patterns of this important plant specialised metabolite pathway.

Materials and Methods

Plant material and sample preparation

Catharanthus roseus (L.) G Don (cv Equator White Eye) was grown at 25°C under 14 h : 10 h, light : dark white fluorescent light photoperiod in a growth chamber (Nippon Medical & Chemical Instruments Co., Osaka, Japan). Seeds were purchased from Sakata Seed Corporation. Leaf tissues of *C. roseus* were harvested from *c.* 3-month-old plants just before Imaging MS, single-cell MS and chloroform dipping experiments. *Catharanthus roseus* (L.) G Don (cv Little bright eye) was grown at 25–30°C under 12 h : 12 h, light : dark for using VIGS analysis.

Observation of idioblast cells and laticifer cells with microscope

Bright field and epifluorescence microscopy were performed on a Leica M205FA microscope (Leica Microsystems, Wetzlar, Germany). Ultraviolet long pass filter (ET UV LP, Leica Microsystems) was used as the epifluorescence filter for observation of idioblast cells and laticifer cells.

Extraction of TIAs from leaf tissues

Catharanthus roseus leaf tissues were frozen with liquid nitrogen immediately after harvesting and ground to fine powder by frost shattering with Multibeads shocker (Yasui Kikai Co., Osaka, Japan). Metabolites were extracted from the powdered sample with 1 ml extraction solution (0.5% formic acid and 1 ppm vindoline-d3 in methanol). Samples were lyophilised with a freeze-dryer (Model 77400; Labconco Co., Kansas City, MO, USA) and stored at −80°C until measurement. Samples were resuspended in methanol.

Liquid chromatography-mass spectrometry (LC-MS) analysis

Crude extracts of leaf tissues were analysed by LC-MS (Prominence, Shimadzu Corp., Kyoto, Japan). The mobile phases A and B were 25 mM ammonium acetate and acetonitrile, respectively. The ratio of solvent A to B was isocratic at 20 : 80. TIAs were separated by reverse-phase octadecylsilyl (ODS) column (Zorbax Eclipse XDB-C18, 5 μm, 4.6 × 150 mm, Agilent Technologies, Santa Clara, CA, USA) for 40 min. The flow rate was 0.25 ml min^{-1} at 40°C. We used vindoline-d3 as an internal standard for quantification of TIA intermediates. Mass spectrometric detection was performed on LTQ Orbitrap (LTQ Orbitrap Velos Pro; Thermo Fisher Scientific, Waltham, MA, USA) mounted on electrospray ionisation (ESI) ion source. The spray voltage for positive measurement was 3800 V. Target mass peaks were detected in ± 5 ppm. We also conducted MS/MS analysis in each TIA peak. Because we could not obtain demethoxyvindoline standard, we cited the MS/MS fragments of demethoxyvindoline measured by Zhou *et al.* (2005).

Chemicals

Commercially available TIA standards, that is catharanthine (Enzo Life Sciences, Farmingdale, NY, USA), tabersonine HCl (AvaChem Scientific, San Antonio, TX, USA), ajmalicine (AdipoGen Life Sciences, Liestal, Switzerland), serpentine hydrogen tartrate (ChromaDex, Irvine, CA, USA), deacetylvindoline (Toronto Research Chemicals, Ontario, Canada), vindoline (ChromaDex) and vindoline-d3 (Toronto Research Chemicals) were used as standards. Strictosidine was produced in Dr Sarah E. O'Connor's laboratory (John Innes Centre). One ppm solutions of these chemicals were used as standards in LC-MS/MS analysis with LTQ Orbitrap (LTQ Orbitrap Velos Pro; Thermo Fisher Scientific) used for the single-cell MS (MS/MS) analysis.

Imaging mass spectrometry

Cross-sections (80 μm thickness) of *C. roseus* first leaf (*c.* 1 cm) including laticifer and/or idioblast cells were prepared with a microtome (Plant Microtome MTH-1; Nippon Medical & Chemical Instruments Co.) and visually inspected with a fluorescence stereoscopic microscope (M205FA; Leica Microsystems). It was difficult to obtain better sections including idioblast cells or laticifer cells from older leaves. Suitable sections were then washed with MilliQ water to remove alkaloid contamination from dead cells and mounted on Indium Tin Oxide (ITO) glass slides (Luminescence Technology Co., Hsin-Chu, Taiwan) using Cryoglue type I (Section-Lab Co. Ltd, Hiroshima, Japan). MilliQ water was added to samples on glass slides in order to prevent sample sections from shrinking before freeze drying. Then, samples were lyophilised by freeze drying (Model 77400, Labconco Co.), taking fluorescence images under microscopy (M205FA, Leica Microsystems) and sublimated by α-cyano-4-hydroxycinnamic acid (CHCA) with a conductive glass using a sublimation apparatus (ChemGlass CG-3038, ChemGlass Life Sciences, Vineland, NJ, USA). Mass spectrometric detection was performed on FT-ICR MS (APEX-Qe 9.4T with dual source; Bruker Daltonics, Billerica, MA, USA). The spatial resolution of Imaging MS was 10–20 μm. MS images were reconstituted using Lab-MSI. Target mass peaks were detected in ± 3 ppm. We judged that the peaks showing > 3 of S/N are reliable. Using this system, we can distinguish real peaks of substances from noise data even the lower amounts of certain substances (Figs S1, S2; Takahashi *et al.*, 2015). We checked the spectrum from each pixel which we could distinguish the types of cells (Fig. S3).

Single-cell MS in leaf tissue

To identify cell-specific alkaloid localisations, we used live single-cell video-mass spectrometry, termed 'single-cell MS' analysis. Cross-sections (100 μm thickness) of the leaf were prepared with a microtome (Plant Microtome MTH-1; Nippon Medical & Chemical Instruments Co.), washed with ultrapure water to remove alkaloid contamination, and then specimens were mounted on a glass slide fixed with double-faced adhesive tape and monitored with a stereomicroscope (M205FA; Leica

Microsystems). The contents of single cells from eight different kinds of cell types, namely IPAP, leaf epidermal cell (LEC), palisade tissue parenchyma cell (PTPC), spongy tissue parenchyma cell (STPC), palisade tissue idioblast cell (PTIC), spongy tissue idioblast cell (STIC), leaf laticifer cell (LLC) and leaf primordium laticifer cell (LPLC), were sucked into a metal/platinum-coated glass capillary nano-electrospray tip (Humanix, Hiroshima, Japan) via tubing using a syringe under the stereoscopic microscope. After the addition of 3 µl of ionisation solvent (0.5% formic acid and 1 ppm vindoline-d3 in methanol) into the nano-electrospray tip from the bottom, the tip was set on a nano-ESI ion source attachment. Mass spectrometric detection was performed on an LTQ Orbitrap Velos Pro instrument. The spray voltage for positive measurement was 1000 V. Alkaloid detection was mainly performed in the range *m/z* 100–1000. The spectrometer was calibrated with poly-tyrosine before experiments. Data analysis was conducted by using XCALIBUR software. Target mass peaks were detected within ± 5 ppm, compared with the theoretical mass. As no isomers of *m/z* 349.15, 389.14, 399.22, 415.22, 427.22, 457.23 and 531.23 ion peaks were found in the extract of whole leaf tissue by LC-MS analysis (Yamamoto *et al.*, 2016), we quantified these alkaloids in each of the eight kinds of cell type by semiquantitative calculation using single-cell MS data on *m/z* intensity values of above ion peaks. When we compared the contents of TIA in laticifer cells between leaf primordium and leaf, the peak intensities of TIAs were corrected with values of the vindoline-d3 ion intensities.

Semiquantitative calculation of single-cell MS was conducted under assumption that the total ion of each cell is almost the same and it was composed of ions of mainly alkaloids.

VIGS of T16H2 and whole leaf imaging

Silencing of T16H2 was achieved by cloning a 252-bp portion of the gene into the pTRV2u vector as reported by Besseau *et al.* (2013). The resulting construct and the empty vector were used for the VIGS assay as described by Liscombe and O'Connor (Liscombe & O'Connor, 2011). Leaves were subjected to metabolite analysis and Imaging MS.

LC-MS analysis of leaf extracts was performed on a Shimadzu IT-TOF instrument coupled to a Nextera X2 UPLC system. Chromatography was performed on a Phenomenex Kinetex 5 µm C18 100 Å (100 × 2.10 mm × 5 µm) kept at 40°C and the binary solvent system consisted of acetonitrile (ACN) and 0.1% formic acid in water. Flow rate was 0.6 ml min^{-1} and the gradient profile was 0 min, 10% ACN; 5 min gradient up to 30% ACN; 6 min gradient up to 100% ACN; 7.5 min isocratic 100% ACN; 8 min back to 0% ACN; 10 min column conditioning at 10% ACN. MS acquisition was performed in positive ion mode in the range *m/z* 150–1200.

Leaf samples used for the imaging experiments were attached to glass slides with double-sided tape, dried overnight under vacuum and then coated with CHCA using a MALDI spotter (SunChrome, Friedrichsdorf, Germany). Imaging MS was performed on a Synapt G2si (Waters, Milford, MA, USA) instrument using MASSLYNX 4.1 and HDI 1.3.5 software. The instrument was calibrated with red phosphorous and acquisition was performed in positive mode in the range *m/z* 50–1200. Acquisition was performed in sensitivity mode with a scan rate of 0.5 s. Laser energy was set to 200. Data were calibrated during the acquisition using a lock mass (red phosphorous) acquired for 5 s every 450 s of acquisition time. Images were collected at 100 µm resolution.

Chloroform dipping of *C. roseus* leaves

Catharanthus roseus young leaves were dipped in 3 ml chloroform in 10 ml glass vials for 30 min in room temperature in order to obtain surface TIAs (Roepke *et al.*, 2010). The chloroform extract was dried with rotary evaporator. Then the chloroform extracted leaves were dipped in 3 ml methanol for 30 min and dried with rotary evaporator. Both extracts were dissolved in 2 ml methanol including 1 ppm ajmaline, filtered with 0.22 µm filters before measurements with LC-MS (IT-TOF, Shimadzu Corp.). After *C. roseus* leaves were dipped in MilliQ or chloroform for 30 min, those leaves were observed under UV with microscopy (DM6000; Leica Microsystems).

Feature detection using principal component analysis (PCA)

Representative spots for each cellular type were chosen based on MS image data or the collection point in single-cell MS measurements, and at least three biological replicates. MS spectra of selected spots from the Imaging MS were converted to plain text files using Bruker or Thermo software. Spectra from each of the spots was merged together using an in-house built binning algorithm (https://github.com/crdzl/MS-binning) programmed in R (https://www.R-project.org/) that iteratively: (1) takes the highest intensity *m/z* peak in all files; (2) collects the peaks within 5 ppm or 0.01 Th (Thomson) in all files as the same feature; and (3) moves to the next higher intensity peak that has not been assigned as a feature. The result is a matrix of intensities with unique *m/z* features as rows, and as many columns as samples. Only features detected in at least one sample with an intensity > 1e5 were kept. The intensity matrix was $\log_{10}$-transformed and quantile-normalised using the preprocessCore (https://github.com/bmbolstad/preprocessCore) library in R, then centred and scaled feature-wise previous to the Analysis of Variance (ANOVA) and PCA. False discovery rate (FDR) correction was calculated using the Benjamini and Hochberg method (Benjamini & Hochberg, 1995). All calculations were performed using the R *stats* library, unless otherwise specified.

Results

Localisation of idioblast cells and laticifer cells in leaf tissue of *C. roseus*

Catharanthus roseus leaf tissue is composed of various types of cells: LPLC, IPAP, LEC, PTPC, STPC, PTIC, STIC, LLC (Fig. 1b,c). In the leaf cross-sections, idioblast cells seemed to exist in parenchyma tissues without a defined pattern and elongated laticifer cells were localised near the vascular bundles

(xylem) (Fig. 1b,c). Idioblast cells and laticifer cells were easily distinguishable from parenchyma cells by blue autofluorescence emitted from the chemical compounds accumulated in these cells when the specimen was excited by UV (Mersey & Cutler, 1986; Carqueijeiro *et al.*, 2016). The autofluorescence of laticifer cells, which is derived mainly from the TIA serpentine, was already observed in leaf primordium (Fig. 1b). Morphogenesis of both idioblast cells and laticifer cells started at the leaf primordium and the number of idioblast cells and laticifer cells increased as the leaf expanded (Fig. 1b).

Imaging MS analysis in leaf cross-section

When we investigated the localisation of TIAs in *C. roseus* stem tissue with Imaging MS (Yamamoto *et al.*, 2016), the 20 μm spatial resolution used provided sufficient resolution, because the size of cells in the stem tissue are relatively large. However, the diameter of leaf cells, such as epidermal cells, is *c.* 10 μm. When we measured leaf tissues with 20 μm spatial resolution of Imaging MS, we could approximately identify localisation of those compounds in leaf sections, but it was difficult to distinguish localisation of TIAs to specific cell types (Fig. 2). Although it was difficult to detect most of alkaloids obtained by 20 μm spatial resolution, we successfully studied the localisation of some TIAs in the leaf tissue precisely by improving the spatial resolution of Imaging MS analysis to 10 μm by adjusting laser diameter and strength (Figs 2, S4–S6). By comparing with the data obtained from a leaf section measured with 20 μm spatial resolution, we succeeded in detecting various TIA compounds in leaf tissue precisely, although total ions created by MALDI ionisation decreased, resulting in decreased detection sensitivity (Fig. 2). As a positive control, we showed the IMS image of a substance (*m/z* 228.0051), which would be detected over the whole figure, although it was difficult to ensure that substances were localised everywhere across the tissues equally.

In this experiment, we detected that the loganic acid (*m/z* 415.1001) as a potassium adduct was highly localised both near the vascular bundle and epidermal cells (Figs 2, S4c). Previous reports based on *in situ* hybridisation and other experiments suggested that catharanthine, strictosidine, loganin and secologanin localised in the epidermal cells (Guirimand *et al.*, 2010, 2011; Roepke *et al.*, 2010). Although it has been proposed that most TIAs were synthesised in the epidermal cells (Fig. 1a; St-Pierre *et al.*, 1999; Guirimand *et al.*, 2011; Pan *et al.*, 2016), MS images revealed that various TIAs, including vindoline (*m/z* 457.2333) and serpentine (*m/z* 349.1546), ultimately accumulated not in the epidermal cells but in the idioblast cells and laticifer cells (Fig. 2). Catharanthine (*m/z* 337.1910) and vindoline were of particular interest, as these compounds are the direct precursors to the antitumour drugs vinblastine and vincristine (Fig. 1a).

Previous work in other laboratories have used chloroform dipping of leaves to define whether alkaloids are localised to the epidermis, but we had inconsistent results between chloroform dipping measurement and our single-cell metabolome analyses. Their results showed that a major alkaloids catharanthine was > 95-% localised in the wax layer (Roepke *et al.*, 2010; PNAS). As a positive control, we checked that we could detect the localisation of ursolic acid in the wax layer with Imaging MS, because it has been reported that ursolic acid localised in wax layer (Usia *et al.*, 2005). We then demonstrated that catharanthine localises not only in the wax layer but also in idioblast and laticifer cells (Figs 2, S4–S6).

Single-cell MS analysis in leaf tissue

In order to obtain quantitative data and MS/MS spectrum data of various TIAs that corroborate the results of Imaging MS, we conducted single-cell MS analyses on internal phloem-associated parenchyma cell (IPAP), LEC, PTPC, STPC, PTIC, STIC, LLC, and LPLC (Figs 1b,c, 3). When we previously measured the contents of a single cell in *C. roseus* stem tissue, we noticed an unstable ionisation time because of matrix effects, which means that the detection time decreased the intensities of peaks. Each single-cell MS spectrum fluctuated due to the matrix effects with direct infusion. In this study, we developed a method in which we added an external standard in elution buffer (1 ppm vindoline-d_3 was resolved in 0.5% formic acid in methanol) to correct the observational error dependent on single-cell MS analysis.

We conducted targeted mass analysis of *C. roseus* TIAs using single-cell MS and LC-MS data (Figs S7–12; Tables 1, S1). The mass spectra of idioblast cells and laticifer cells showed that major TIA peaks including catharanthine (*m/z* 337.19), serpentine (*m/z* 349.15) and vindoline (*m/z* 457.23) were detected as primary peaks in those spectra. Catharanthine (*m/z* 337.19) was also detected in the mass spectra of parenchyma cells and epidermal cells. As for catharanthine, we needed further measurements, where the majority of catharanthine was secreted from epidermal cells, to compare this in idioblast cells and laticifer cells (Fig. S13). Therefore, we performed MS/MS analyses of the peak at *m/z* 337.19 to clarify whether this was catharanthine, tabersonine or another isomeric alkaloid (Table S2). As a result of MS/MS, a catharanthine-specific fragment peak (*m/z* 93.07) from all types of cells showing *m/z* 337.19 was detected (Tables 1, S2; Yamamoto *et al.*, 2016). MS/MS fragments corresponding to serpentine (*m/z* 349.15) and vindoline (*m/z* 457.23) were detected in single-cell MS and LC-MS/MS analyses (Tables 1, S2; Fig. 3; Yamamoto *et al.*, 2016). Moreover, we speculated on the possible TIA identities of several other peaks (Table S1). To determine whether these peaks were real TIAs, their MS/MS fragments were analysed in a similar manner previously reported with stem tissue (Table S2; Yamamoto *et al.*, 2016).

Principal component analysis (PCA) of Imaging MS and single-cell MS data

PCA was conducted with MS image data and single-cell MS data (Figs S14, S15). These PCA data showed that idioblast and laticifer cell had many similar features, especially many alkaloid peaks, that is *m/z* 349.15, 427.22 and 457.23, localised in idioblast cells and laticifer cells. Regarding strictosidine (*m/z* 531.23), this compound was also localised in epidermal cells. These PCA data also showed that secologanin was (*m/z* 427.10) highly localised in epidermal cells.

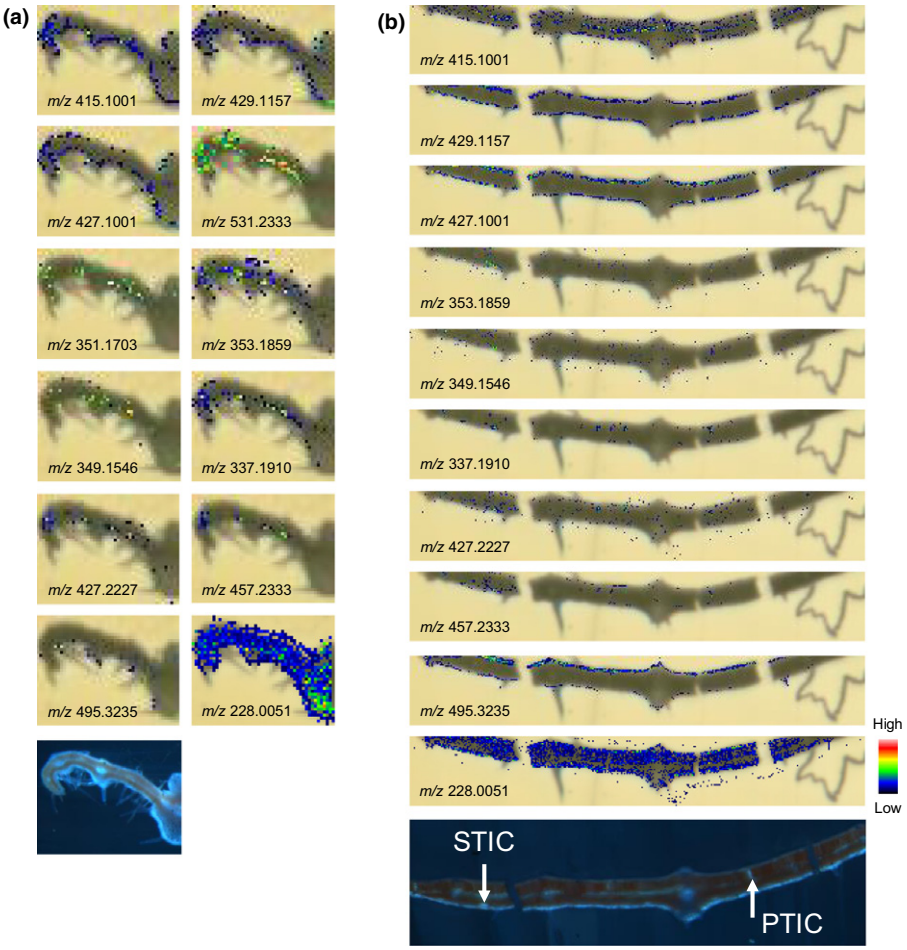

Fig. 2 Imaging MS analysis in leaf tissue. (a) MS images of *Catharanthus roseus* leaf cross-section measured with 20 μm spatial resolution. *m/z* 415.1001 ([M+K]+ loganic acid), *m/z* 429.1157 ([M+K]+ loganin), *m/z* 427.1001 ([M+K]+ secologanin), *m/z* 531.2333 ([M+H]+ strictosidine), *m/z* 351.1703 ([M+H]+ cathenamine), *m/z* 353.1859 ([M+H]+ ajmalicine), *m/z* 349.1546 ([M+H]+ serpentine), *m/z* 337.1910 ([M+H]+ catharanthine), *m/z* 427.2227 ([M+H]+ demethoxyvindoline (vindorosine)), *m/z* 457.2333 ([M+H]+ vindoline), *m/z* 495.3235 ([M+K]+ ursolic acid), *m/z* 228.0051 as a positive control. (b) MS images of *C. roseus* leaf cross-section measured with 10 μm spatial resolution. Most TIA localised in idioblast cell and laticifer cell. *m/z* 415.1001 ([M+K]+ loganic acid), *m/z* 429.1157 ([M+K]+ loganin), *m/z* 427.1001 ([M+K]+ secologanin), *m/z* 353.1859 ([M+H]+ ajmalicine), *m/z* 349.1546 ([M+H]+ serpentine), *m/z* 337.1910 ([M+H]+ catharanthine), *m/z* 427.2227 ([M+H]+ demethoxyvindoline (vindorosine)), *m/z* 457.2333 ([M+H]+ vindoline), *m/z* 495.3235 ([M+K]+ ursolic acid), *m/z* 228.0051 as a positive control. Colour bar represents MS signal intensity. Bottom fluorescence images of cells following UV light excition. PTIC, palisade tissue idioblast cell; STIC, spongy tissue idioblast cell.

Semiquantitative analysis of single-cell MS

The metabolome of *C. roseus* leaf tissue was analysed by using LC-MS. We detected that single peaks at *m/z* 349.15, 389.14, 399.22, 415.22, 427.22, 457.23 and 531.23 correspond to serpentine, secologanin, desacetoxyvindoline, deacetylvindoline, demethoxyvindoline, vindoline and strictosidine, respectively (Table S1). Judging from the LC-MS results, we could deduce that these *m/z* values showed a single molecular species in each cell type of *C. roseus* leaf tissue (Yamamoto *et al.*, 2016). Semiquantitative calculations were made for *m/z* 349.15, 389.14, 399.22, 415.22, 427.22, 457.23 and 531.23 ion peaks from the single-cell MS data measured with mass range *m/z* 100–1000 (Table 1). Most TIAs (349.15 (serpentine), 399.22 (desacetoxyvindoline), 415.22 (deacetylvindoline), 427.22 (demethoxyvindoline), 457.23 (vindoline) and 531.23 (strictosidine)) were accumulated in idioblast cells and laticifer cells (Fig. 3). Secologanin and strictosidine, which have been reported to be produced in the epidermal cells (St-Pierre *et al.*, 1999; Pan *et al.*, 2016), were detected in epidermal cells as well (Fig. 3).

Comparison of semiquantitative data of laticifer cells between leaf primordium and leaf tissue

By using single-cell MS data, we calculated semiquantitatively the amounts of alkaloids in each of the cell types. Although this calculation had some limitation as explained in Methods, we could see that the profiles of specialised metabolites were different among the tissues of *C. roseus* (Figs 3, S7). In previous research, we compared TIA contents in the first leaf pair and the stem tissue using LC-MS/MS (Yamamoto *et al.*, 2016). There was a large difference of vindoline content between these samples, in which the first leaf sample accumulated more vindoline and its intermediates than the stem tissue (Yamamoto *et al.*, 2016). To detect intermediates of the vindoline biosynthetic pathway in the first leaf, we measured the contents of laticifer cells with single-cell MS, which were suspected to start to accumulate vindoline in the leaf primordium (Fig. 3). In fact, although we succeeded in detecting a much higher amount of vindoline in the laticifer cells in leaf tissue, the metabolome data of laticifer cells in the leaf primordium showed less accumulation of vindoline (Fig. 3).

T16H2 is related to vindoline biosynthesis in *C. roseus* leaf tissue

Metabolome analyses revealed tissue-specific vindoline accumulation in the first pair leaf (Yamamoto *et al.*, 2016). Tabersonine 16-hydroxylase 2 (T16H2) produces 16-hydroxytabersonine, which is the initial intermediate in the vindoline pathway (Fig. 1a). As T16H2 may coordinate differentiation between the vindoline and demethoxyvindoline pathways (Fig. 4; Besseau *et al.*, 2013), we conducted VIGS

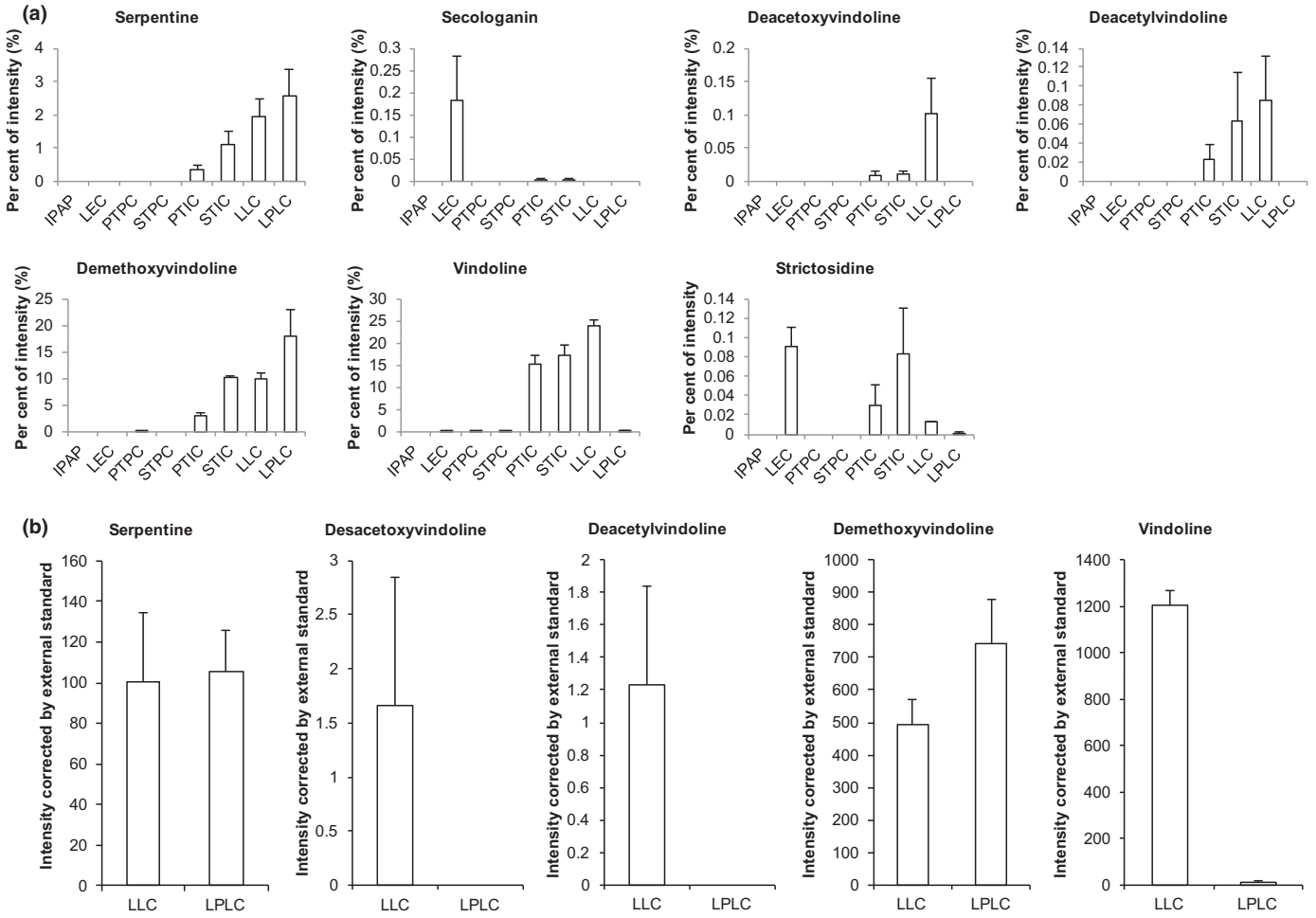

Fig. 3 Single-cell mass spectrometry (MS) analysis in *Catharanthus roseus* leaf tissue. (a) Semiquantitative analysis of terpenoid indole alkaloids (TIAs) calculated by using single-cell MS analysis data. Serpentine ([M+H]+ *m/z* 349.15), secologanin ([M+H]+ *m/z* 389.14), desacetoxyvindoline ([M+H]+ *m/z* 399.22), deacetylvindoline ([M+H]+ *m/z* 415.22), demethoxyvindoline ([M+H]+ *m/z* 427.22), vindoline ([M+H]+ *m/z* 457.23), strictosidine ([M+H]+ *m/z* 531.23). *Y*-axis shows per cent intensity normalised to the total ion intensity value of each sample. Values are the mean of three measurements (±SEM). IPAP, internal phloem-associated parenchyma cell; LEC, leaf epidermal cell; PTPC, palisade tissue parenchyma cell; STPC, spongy tissue parenchyma cell; PTIC, palisade tissue idioblast cell; STIC, spongy tissue idioblast cell; LLC, leaf laticifer cell; LPLC, leaf primordium laticifer cell. (b) TIA contents in leaf laticifer cell (LLC) and leaf primordium laticifer cell (LPLC). Values are the mean of three measurements (±SEM).

Table 1 Terpenoid indole alkaloid (TIA) and iridoid detected in *Catharanthus roseus* leaf tissue using single-cell MS analysis (mass range *m/z* 100–1000).

Molecular formula	[M+H]+	IPAP	LEC	PTPC	STPC	PTIC	STIC	LLC	Speculated compound
C21H24N2O2	337.191054		○			○	○	○	Catharanthine/Tabersonine
C21H20N2O3	349.154668					○	○	○	Serpentine
C21H22N2O3	351.170318					○	○	○	Cathenamine
C21H24N2O3	353.185968					○	○	○	Ajmalicine
C21H26N2O3	355.201618					○	○	○	Stemmadenine
C22H26N2O3	367.201618					○	○	○	16-Methoxytabersonine
C16H24O10	377.144222								Loganic acid
C22H28N2O4	385.212183						○	○	16-Methoxy-2,3-dihydro-3-hydroxytabersonine
C17H24O10	389.144222		○						Secologanin
C17H26O10	391.159873								Loganin
C23H30N2O4	399.227833						○	○	Desacetoxyvindoline
C23H30N2O5	415.222748					○	○	○	Deacetylvindoline
C24H30N2O5	427.222748					○	○	○	Demetoxyvindoline
C25H32N2O6	457.233312					○	○	○	Vindoline
C27H34N2O9	531.233706		○			○	○	○	Strictosidine

Circles○: Chemical compound exists in leaf tissue each cell type ($n = 3$).

analysis of T16H2 to confirm whether gene expression of T16H2 regulates the differences between vindoline and demethoxyvindoline accumulation in expanding leaf tissue (Besseau *et al.*, 2013). This VIGS analysis showed that the silencing of T16H2 led to demethoxyvindoline accumulation in expanding leaf tissue compared with vindoline (Fig. 4). This analysis showed that silencing of T16H2 led to a 14-fold increase in demethoxyvindoline accumulation in leaf tissue compared with nonsilenced plants (EV). The levels of tabersonine were also significantly increased, while the amount of vindoline in the silenced tissues dropped by 2.3-fold (Fig. 4a).

Discussion

TIA production in the leaf tissue of *C. roseus*

LC-MS analysis data of *C. roseus* leaf extracts showed that the major TIAs were catharanthine, vindoline and various vindoline intermediates (Table S1; Yamamoto *et al.*, 2016). To verify the identity of these compounds, we measured authentic standards of commercially available TIAs by MS/MS analysis using the same MS apparatus (Table S2). For compounds with no available standard, such as vindoline intermediates, we obtained MS/MS fragments and detected a skeleton-specific MS/MS fragment (*m/z* 188) diagnostic of the aspidosperma skeleton (Table S2). Interestingly, *m/z* peaks of vindoline intermediates, such as desacetoxyvindoline and deacetylvindoline, were detected as a single peak with LC-MS analysis (Table S1). Based on this MS/MS information, we deduced these TIA peaks as vindoline intermediates.

We were able to confirm that idioblast cells and laticifer cells contained catharanthine, serpentine and ajmalicine, using standard MS/MS fragment data. In the current model of TIA localisation, using data from the *C. roseus* cultivar (cv Little delicata), catharanthine is believed to be transported to the wax layer after biosynthesis in the epidermal cells (Roepke *et al.*, 2010; Yu & De Luca, 2013). To our surprise, from single-cell MS analysis, both stem tissue and leaf tissue contained catharanthine in idioblast cells and laticifer cells as well. It is possible that catharanthine might be transported into idioblast cells and laticifer cells from the epidermal cells.

So far, it is unclear where serpentine, which is the oxidation product of ajmalicine, is produced in *C. roseus* tissues. According to our results, this biosynthesis may occur in idioblast cells and laticifer cells, as these compounds are also localised in idioblast cells and laticifer cells (Fig. 3a).

Improvement of Imaging MS

This study required substantial improvement of spatial resolution of Imaging MS compared with previous reports, because the epidermal cells in leaf tissue are much smaller than cells in the stem tissue (Fig. 1c). When the diameter of the laser for ionisation was changed from 20 μm to 10 μm, the ion intensity induced by laser radiation decreased and consequently we missed several mass spectrometry imaging (MSI) data, which we could detect in Imaging MS with 20 μm spatial resolution. However, after optimisation, we finally succeeded in the detection of certain alkaloids with 10 μm spatial resolution (Fig. 2). These MS images made it possible to distinguish each cell in leaf tissue, where TIAs localised. For example, MS images of *m/z* 457.2333 (vindoline) showed that this compound localised to both PTIC and STIC (Fig. 2b).

Cell-specific localisation of TIAs in leaf tissue

The current model for TIA biosynthesis is that synthesis initially occurs in IPAP cells and then the products move from IPAP cells to epidermal cells, parenchyma cells, idioblast cells and laticifer cells (St-Pierre *et al.*, 1999; Burlat *et al.*, 2004; Mahroug *et al.*, 2007; Guirimand *et al.*, 2011; Pan *et al.*, 2016). It has been proposed that loganic acid is the iridoid intermediate that is transferred from IPAP cells to epidermal cells and desacetoxyvindoline from epidermal cells to other cells (Fig. 1). This hypothesis is based on *in situ* hybridisation data and localisation of mRNAs of genes encoding enzymes involved in TIA biosynthesis (Dugé de Bernonville *et al.*, 2015; Pan *et al.*, 2016). The localisation of actual TIA molecules at the cellular level has been never detected (Mersey & Cutler, 1986).

Imaging MS data showed that loganin (*m/z* 429.1157) and secologanin (*m/z* 427.1001) localised in the epidermal cells (Fig. 2a,b). Single-cell MS showed the same localisation as for secologanin (*m/z* 389.14) (Fig. 3a). Unfortunately, loganin was not detected using single-cell MS as a proton adduct, because the ionisation efficiency of this compound decreases when using ESI. However, we succeeded in detecting secologanin and loganin as sodium adducts using ESI (Table S3). Moreover, these iridoid metabolites have previously been shown to be synthesised in the epidermal cells of *C. roseus* tissues (Dugé de Bernonville *et al.*, 2015), and this was also confirmed by our former analysis in stem tissue (Yamamoto *et al.*, 2016).

We were also not able to detect the immediate precursor to loganin, loganic acid, in single-cell MS analysis. Although we could not semiquantify this substance, we concluded that loganic acid localised in both IPAP cells and epidermal cells, according to MS image of *m/z* 415.1001 (loganic acid) (Fig. 2). This is consistent with the substrate specificity of a newly discovered iridoid transporter that appears to have broad specificity for a number of iridoid intermediates (7-deoxyloganic acid, loganic acid, loganin and secologanin) (Larsen *et al.*, 2017).

Imaging MS and single-cell MS data also showed that most TIAs, including catharanthine (*m/z* 337.19), localised in the idioblast cells and the laticifer cells (Table 1; Figs 2, 3). These data contrast with previously published reports that showed catharanthine localised in the wax layer of the leaf tissue (Roepke *et al.*, 2010; Yu & De Luca, 2013). The experiments here suggested that at least some catharanthine also remains within the leaf, in the idioblast and laticifer cells. As for the localisation of catharanthine, Roepke *et al.* (2010) showed that most catharnthine exists in the wax layer outside the leaves, by using chloroform dipping. We have reproduced similar results using the same

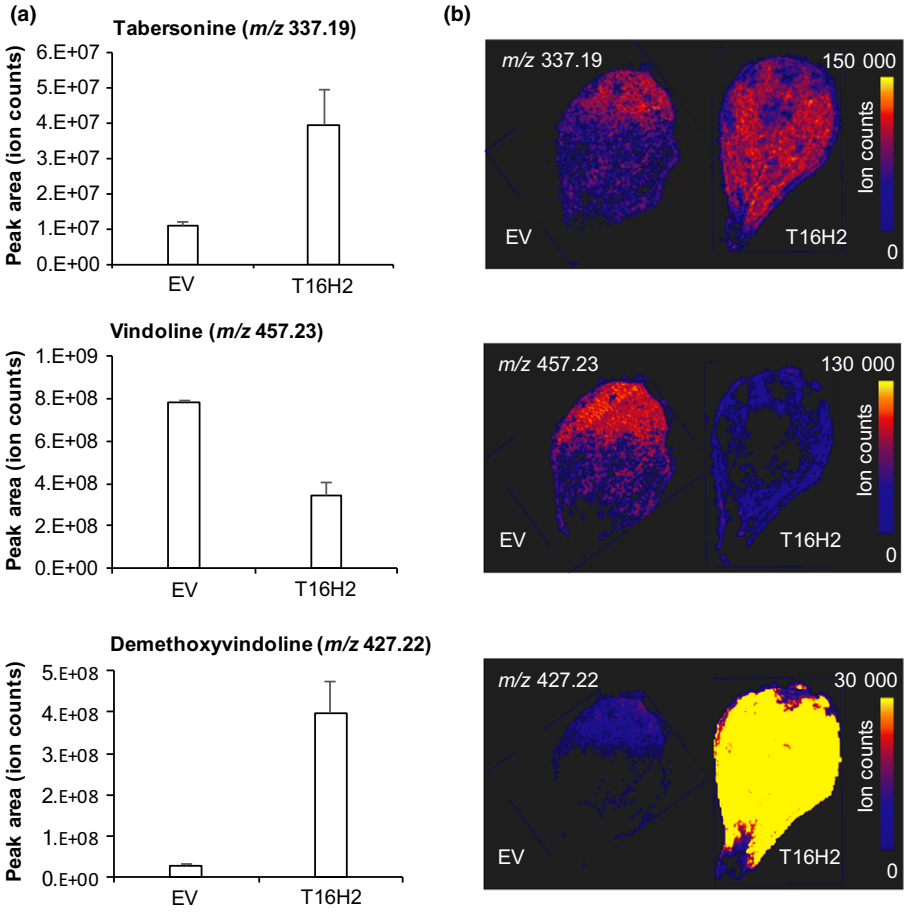

Fig. 4 Vindoline biosynthesis in *Catharanthus roseus* leaf tissue. (a) Peak area of terpenoid indole alkaloid (TIA) between empty vector (EV) samples and T16H2 VIGS samples by LC-MS measurements. Values are the mean of six measurements (±SEM). (b) MS images in EV samples and T16H2 VIGS samples using Imaging MS.
Annotation : catharanthine ([M+H]+ *m/z* 337.19), vindoline ([M+H]+ *m/z* 457.23), demethoxyvindoline ([M+H]+ *m/z* 427.22).

method (Fig. S13). However, we also detected some catharanthine in laticifer and idioblast cells using single-cell MS and MS/MS methods. At present, we cannot explain the difference between these two studies, but further investigation into the localisation of TIA should eventually resolve this complex issue.

Furthermore, our single-cell MS measurements are consistent with a previous report that showed that serpentine, ajmalicine and vindoline accumulated in the fraction of idioblast cells (Mersey & Cutler, 1986; Carqueijeiro *et al.*, 2016; Yamamoto *et al.*, 2016). Additionally, we also showed here that a compound of *m/z* 531.23 (strictosidine) localised not only in the epidermal cells but also in the idioblast cells and laticifer cells (Table 1; Figs 2a, 3a). Strictosidine might be transported from the vacuole in the epidermal cells as soon as it is produced, and accumulates in all cells that have a strictosidine transporter. However, it cannot be excluded that not only final products are transported but also intermediates and that these intermediates accumulate in cells where they are not metabolised. It is also possible that symplasmic transport via plasmodesmata might drive movements of TIA intermediates between adjacent cells (Fig. 5).

Recently, it was revealed that a member of the NPF transporter family was related to strictosidine transport and other members of the NPF family have been implicated in iridoid glucoside transport (Larsen *et al.*, 2017; Payne *et al.*, 2017). It has also been reported that various transporters may be involved in the transport of alkaloids (Carqueijeiro *et al.*, 2013; Shitan *et al.*, 2014). Further studies are needed to clarify how these compounds distribute between the different cell types in *C. roseus*, and how the site of biosynthesis may differ from the site of accumulation.

Changes in vindoline accumulation in laticifer cells depending on leaf stages

The contents of vindoline were substantially different between the stem and leaf tissues (Yamamoto *et al.*, 2016). High levels of accumulation of vindoline in leaf tissue is a major reason why mature leaves are the main source of antitumour drugs. To investigate how vindoline accumulates in *C. roseus* idioblast cells and laticifer cells in the leaf tissue, we also measured laticifer cells localised in the leaf primordium with single-cell MS (Fig. 3). TIA composition in laticifer cells in the leaf primordium was different from that of laticifer cells localised in the first pair leaves (*c.* 1 cm). Although we could detect vindoline in the laticifer cells in leaf primordium, we could not detect any vindoline intermediates, such as desacetoxyvindoline and deacetylvindoline in those cells (Fig. 3). Judging from this result, we would consider that vindoline biosynthesis starts in leaf primordium, but that the laticifer cells in leaf primordium have not accumulated enough vindoline intermediates to detect with single-cell MS measurement.

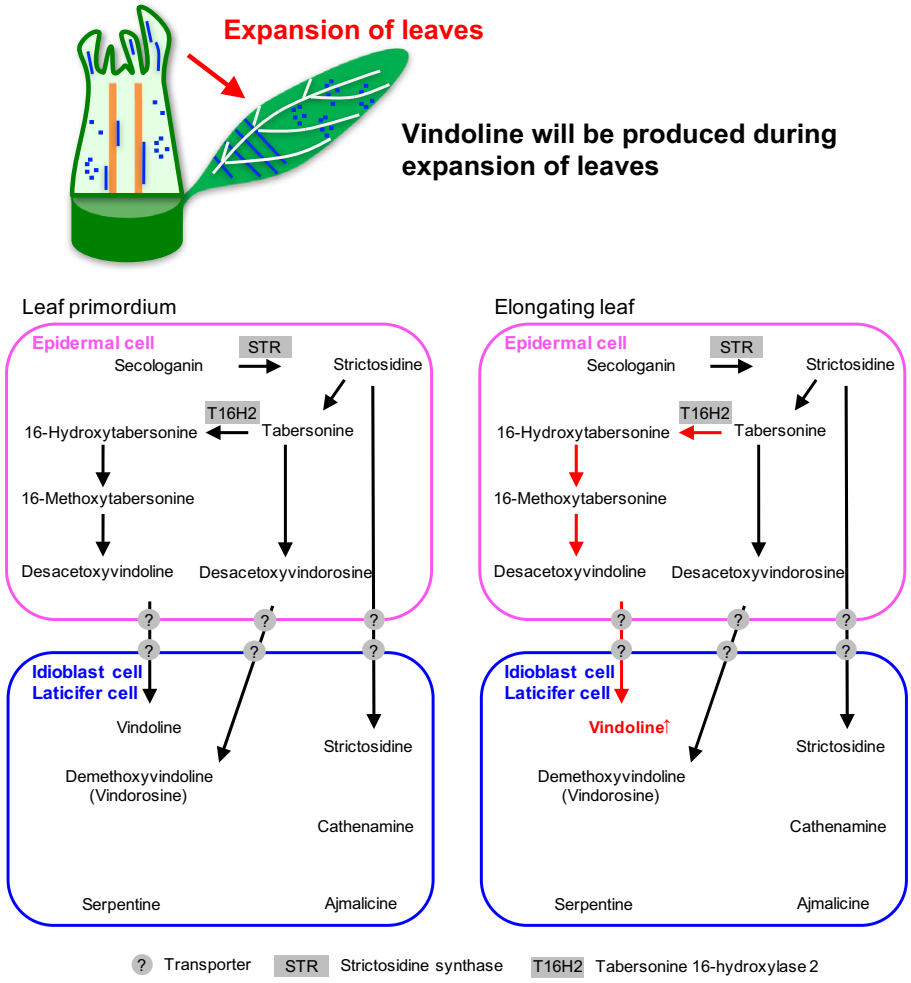

Fig. 5 Cell-specific localisation of terpenoid indole alkaloid (TIA) in *Catharanthus roseus* leaf tissue. Vindoline accumulates in idioblast and laticifer cells of the elongating leaf.

Conversely, the demethoxyvindoline pathway might be continuously activated in stem and leaf primordium (Figs 1a, 5), which is why we could detect demethoxyvindoline in laticifer cells in stem and leaf primordium (Fig. 3; Yamamoto *et al.*, 2016).

Tabersonine 16-hydroxylase 2 (T16H2) regulates the biosynthesis of vindoline and demethoxyvindoline among stem and leaf tissues

The enzymes for biosynthesis of vindoline and demethoxyvindoline from their common starting material, tabersonine, in *C. roseus* have been recently elucidated (Qu *et al.*, 2015). Tabersonine 16-hydroxylase 2 (T16H2) is likely to play a key role in controlling the branch point of these two metabolic pathways (Fig. 1a). Previously reported RNA-seq data suggested that the gene expression of T16H2 is increased in leaf tissue compared with stem tissue, where low amounts of vindoline accumulate (Van Moerkercke *et al.*, 2013, 2015). Furthermore, VIGS analysis of T16H2 led to accumulation of demethoxyvindoline in leaf tissues at the expense of vindoline, further supporting that T16H2 is needed for production of vindoline in leaf tissue. The lack of expression of T16H2 might be a reason why demethoxyvindoline accumulated in idioblast cells and laticifer cells in the stem, instead of vindoline (Yamamoto *et al.*, 2016).

Idioblast and laticifer cells might play important roles in alkaloid biosynthesis

In the present study, we used cutting-edge metabolome analyses, Imaging MS and single-cell MS to detect the types of TIAs that localised in idioblast and laticifer cells in leaf tissue. In our measurement, the idioblast and laticifer cells contained various alkaloids including strictosidine, vindoline and serpentine. Notably, as strictosidine is a central precursor for all TIAs, these data strongly suggested that idioblast and laticifer cells may play important roles in the production of various TIAs. We also found that TIA composition in laticifer cells among stem, leaf primordium and leaf were different. Interestingly, we could not detect any vindoline, or vindoline intermediates such as desacetoxyvindoline and deacetylvindoline in the laticifer cells of stem, but we could detect vindoline in the laticifer cells of leaf primordium and leaf tissue. Those results suggest that the vindoline biosynthetic pathway might function only in expanding leaf.

Overall this study highlights the complexity of specialised metabolism, and strongly suggests that the same biosynthetic intermediates can be located in two spatially distinct places. Undoubtedly, this complexity adds an additional layer of control onto the biosynthesis of these complex molecules. This study highlights that it is crucial to incorporate location of all molecules

– transcripts, proteins and metabolites – into a model of metabolic pathway localisation.

Acknowledgements

We greatly appreciate Dr Tsuyoshi Esaki (National Institutes of Biomedical Innovation, Health and Nutrition) for measurement of single-cell MS, Dr Akio Murakami (Kobe University) for his kind support in preparing the manuscript. This work was partly supported by MEXT KAKENHI Grant 22120006 (to TMimura) and JSPS KAKENHI Grants 14J03616 (to KY) and 24710235 (to MO).

Author contributions

KY and TMimura planned and coordinated the project and wrote the manuscript. KY and TMimura designed the research. KY, HM and TMasujima performed single-cell MS analysis. KY and KT performed Imaging analysis. LC and SEO performed VIGS analysis. HM, CER-L, TI, MO, KI, HF and MY helped to prepare the manuscript and to analyse data.

ORCID

Hidehiro Fukaki https://orcid.org/0000-0002-6251-7668
Kimitsune Ishizaki https://orcid.org/0000-0003-0504-8196
Kotaro Yamamoto https://orcid.org/0000-0003-3817-333X

References

Benjamini Y, Hochberg Y. 1995. Controlling the false discovery rate: a practical and powerful approach to multiple testing. *Journal of the Royal Statistical Society Series B* **57**: 289–300.

Besseau S, Kellner F, Lanoue A, Thamm AM, Salim V, Schneider B, Geu-Flores F, Höfer R, Guirimand G, Guihur A *et al.* 2013. A pair of tabersonine 16-hydroxylases initiates the synthesis of vindoline in an organ-dependent manner in *Catharanthus roseus*. *Plant Physiology* **163**: 1792–1803.

Burlat V, Oudin A, Courtois M, Rideau M, St-Pierre B. 2004. Co-expression of three MEP pathway genes and geraniol 10-hydroxylase in internal phloem parenchyma of *Catharanthus roseus* implicates multicellular translocation of intermediates during the biosynthesis of monoterpene indole alkaloids and isoprenoid-derive. *The Plant Journal* **38**: 131–141.

Carqueijeiro I, Guimarães AL, Bettencourt S, Martínez-Cortés T, Guedes JG, Gardner R, Lopes T, Andrade C, Bispo C, Martins NP *et al.* 2016. Isolation of cells specialized in anticancer alkaloid metabolism by fluorescence activated cell sorting. *Plant Physiology* **171**: 2371–2378.

Carqueijeiro I, Noronha H, Duarte P, Geros H, Sottomayor M. 2013. Vacuolar transport of the medicinal alkaloids from *Catharanthus roseus* is mediated by a proton-driven antiport. *Plant Physiology* **162**: 1486–1496.

Dugé de Bernonville T, Clastre M, Besseau S, Oudin A, Burlat V, Glévarec G, Lanoue A, Papon N, Giglioli-Guivarc'h N, St-Pierre B *et al.* 2015. Phytochemical genomics of the Madagascar periwinkle: unravelling the last twists of the alkaloid engine. *Phytochemistry* **113**: 9–23.

Fujii T, Matsuda S, Tejedor ML, Esaki T, Sakane I, Mizuno H, Tsuyama N, Masujima T. 2015. Direct metabolomics for plant cells by live single-cell mass spectrometry. *Nature Protocols* **10**: 1445–1456.

Gigant B, Wang C, Ravelli RB, Roussi F, Steinmetz MO, Curmi PA, Sobel A, Knossow M. 2005. Structural basis for the regulation of tubulin by vinblastine. *Nature* **435**: 519–522.

Guirimand G, Courdavault V, Lanoue A, Mahroug S, Guihur A, Blanc N, Giglioli-Guivarc'h N, St-Pierre B, Burlat V. 2010. Strictosidine activation in Apocynaceae: towards a 'nuclear time bomb'? *BMC Plant Biology* **10**: 182.

Guirimand G, Guihur A, Ginis O, Poutrain P, Héricourt F, Oudin A, Lanoue A, St-Pierre B, Burlat V, Courdavault V. 2011. The subcellular organization of strictosidine biosynthesis in *Catharanthus roseus* epidermis highlights several trans-tonoplast translocations of intermediate metabolites. *FEBS Journal* **278**: 749–763.

Kavallaris M. 2010. Microtubules and resistance to tubulin-binding agents. *Nature Reviews Cancer* **10**: 194–204.

Larsen B, Fuller VL, Pollier J, Van Moerkercke A, Schweizer F, Payne R, Colinas M, O'Connor SE, Goossens A, Halkier BA. 2017. Identification of iridoid glucoside transporters in *Catharanthus roseus* transport iridoid glucosides. *Plant and Cell Physiology* **58**: 1507–1518.

Liscombe DK, O'Connor SE. 2011. A virus-induced gene silencing approach to understanding alkaloid metabolism in *Catharanthus roseus*. *Phytochemistry* **72**: 1969–1977.

Mahroug S, Burlat V, St-Pierre B. 2007. Cellular and sub-cellular organisation of the monoterpenoid indole alkaloid pathway in *Catharanthus roseus*. *Phytochemistry Reviews* **6**: 363–381.

Mahroug S, Courdavault V, Thiersault M, St-Pierre B, Burlat V. 2006. Epidermis is a pivotal site of at least four secondary metabolic pathways in *Catharanthus roseus* aerial organs. *Planta* **223**: 1191–1200.

Mersey BG, Cutler AJ. 1986. Differential distribution of specific indole alkaloids in leaves of *Catharanthus roseus*. *Canadian Journal of Botany* **64**: 1039–1045.

Mizuno H, Tsuyama N, Harada T, Masujima T. 2008. Live single-cell video-mass spectrometry for cellular and subcellular molecular detection and cell classification. *Journal of Mass Spectrometry* **43**: 1692–1700.

Murata J, Roepke J, Gordon H, De Luca V. 2008. The leaf epidermome of *Catharanthus roseus* reveals its biochemical specialization. *Plant Cell* **20**: 524–542.

O'Keefe BR, Mahady GB, Gills JJ, Beecher CWW, Schilling AB. 1997. Stable vindoline production in transformed cell cultures of *Catharanthus roseus*. *Journal of Natural Products* **60**: 261–264.

Pan Q, Mustafa NR, Tang K, Choi YH, Verpoorte R. 2016. Monoterpenoid indole alkaloids biosynthesis and its regulation in *Catharanthus roseus*: a literature review from genes to metabolites. *Phytochemistry Reviews* **15**: 221–250.

Payne RM, Xu D, Foureau E, Teto Carqueijeiro MI, Oudin A, Bernonville TD, Novak V, Burow M, Olsen CE, Jones DM *et al.* 2017. An NPF transporter exports a central monoterpene indole alkaloid intermediate from the vacuole. *Nature Plants* **3**: 16208.

Qu Y, Easson ML, Froese J, Simionescu R, Hudlicky T, De Luca V. 2015. Completion of the seven-step pathway from tabersonine to the anticancer drug precursor vindoline and its assembly in yeast. *Proceedings of the National Academy of Sciences, USA* **112**: 6224–6229.

Roepke J, Salim V, Wu M, Thamm AM, Murata J, Ploss K, Boland W, De Luca V. 2010. Vinca drug components accumulate exclusively in leaf exudates of Madagascar periwinkle. *Proceedings of the National Academy of Sciences, USA* **107**: 15287–15292.

Shitan N, Kato K, Shoji T. 2014. Alkaloid transporters in plants. *Plant Biotechnology* **31**: 453–463.

St-Pierre B, Vazquez-Flota FA, De Luca V. 1999. Multicellular compartmentation of *Catharanthus roseus* alkaloid biosynthesis predicts intercellular translocation of a pathway intermediate. *Plant Cell* **11**: 887–900.

Takahashi K, Kozuka T, Anegawa A, Nagatani A, Mimura T. 2015. Development and application of a high-resolution imaging mass spectrometer for the study of plant tissues. *Plant and Cell Physiology* **56**: 1329–1338.

Usia T, Watabe T, Kadota S, Tezuka Y. 2005. Cytochrome P450 2D6 (CYP2D6) inhibitory constituents of *Catharanthus roseus*. *Biological and Pharmaceutical Bulletin* **28**: 1021–1024.

Van der Heijden R, Jacobs DI, Snoeijer W, Hallard D, Verpoorte R. 2004. The *Catharanthus* alkaloids: pharamacognosy and biochemistry. *Current Medicinal Chemistry* **11**: 607–628.

Van Moerkercke A, Fabris M, Pollier J, Baart GJ, Rombauts S, Hasnain G, Rischer H, Memelink J, Oksman-Caldentey KM, Goossens A. 2013. CathaCyc, a metabolic pathway database built from *Catharanthus roseus* RNA-seq data. *Plant and Cell Physiology* **54**: 673–685.

Van Moerkercke A, Steensma P, Schweizer F, Pollier J, Gariboldi I, Payne R, Vanden Bossche R, Miettinen K, Espoz J, Purnama PC *et al.* 2015. The bHLH transcription factor BIS1 controls the iridoid branch of the monoterpenoid indole alkaloid pathway in *Catharanthus roseus*. *Proceedings of the National Academy of Sciences, USA* **112**: 8130–8135.

Verma P, Mathur AK, Srivastava A, Mathur A. 2012. Emerging trends in research on spatial and temporal organization of terpenoid indole alkaloid pathway in *Catharanthus roseus*: a literature update. *Protoplasma* **249**: 255–268.

Yamamoto K, Takahashi K, Mizuno H, Anegawa A, Ishizaki K, Fukaki H, Ohnishi M, Yamazaki M, Masujima T, Mimura T. 2016. Cell-specific localization of alkaloids in *Catharanthus roseus* stem tissue measured with Imaging MS and single-cell MS. *Proceedings of the National Academy of Sciences, USA* **113**: 3891–3896.

Yoder LR, Mahlberg PG. 1976. Reactions of alkaloid and histochemical indicators in laticifers and specialized parenchyma cells of *Catharanthus roseus* (Apocynaceae). *American Journal of Botany* **63**: 1167–1173.

Yu F, De Luca V. 2013. ATP-binding cassette transporter controls leaf surface secretion of anticancer drug components in *Catharanthus roseus*. *Proceedings of the National Academy of Sciences, USA* **110**: 15830–15835.

Zhou H, Tai Y, Sun C, Pan Y. 2005. Rapid identification of vinca alkaloids by direct-injection electrospray ionisation tandem mass spectrometry and confirmation by high-performance liquid chromatography – Mass spectrometry. *Phytochemical Analysis* **16**: 328–333.

Supporting Information

Additional Supporting Information may be found online in the Supporting Information section at the end of the article.

Fig. S1 Data analysis of MSI data (*m/z* 457.2333) with in-house software.

Fig. S2 Data analysis of MSI data (*m/z* 427.2227) with in-house software.

Fig. S3 Example of Imaging MS spectrum in each measurement spot.

Fig. S4 Comparison MSI data among proton adduct, sodium adduct and potassium adduct.

Fig. S5 MSI data of *C. roseus* leaf tissue samples 1.

Fig. S6 MSI data of *C. roseus* leaf tissue samples 2.

Fig. S7 Single-cell MS spectrum of each cell types.

Fig. S8 Single-cell MS/MS spectrum of PTIC.

Fig. S9 Single-cell MS/MS spectrum of LLC.

Fig. S10 Single-cell MS/MS spectrum of LEC.

Fig. S11 Single-cell MS/MS data of *m/z* 337.1 compared with catharanthine and tabersonine standards.

Fig. S12 Quantitative data of each cell type with single-cell MS data.

Fig. S13 Chloroform dipping analysis of *C. roseus* leaf.

Fig. S14 PCA of Imaging MS data.

Fig. S15 PCA of single-cell MS data.

Table S1 TIA detected by LC-MS analysis of *C. roseus* leaf tissue samples.

Table S2 MS/MS spectrum in *C. roseus* leaf tissue.

Table S3 Iridoid detected using single-cell MS analysis (mass range *m/z* 100–1000).

Please note: Wiley Blackwell are not responsible for the content or functionality of any Supporting Information supplied by the authors. Any queries (other than missing material) should be directed to the *New Phytologist* Central Office.